PHYSICAL REVIEW D **87,** 013010 (2013)

Supersymmetric type-III seesaw mechanism: Lepton flavor violation and LHC phenomenology

M. Hirsch*

AHEP Group, Instituto de Física Corpuscular—C.S.I.C./Universitat de València Edificio de Institutos de Paterna, Apartado 22085, E-46071 València, Spain

W. Porod† and Ch. Weiß‡

Institut für Theoretische Physik und Astronomie, Universität Würzburg Am Hubland, 97074 Wuerzburg, Germany

F. Staub§

Bethe Center for Theoretical Physics & Physikalisches Institut der Universität Bonn, Nußallee 12, 53115 Bonn, Germany

(Received 8 November 2012; published 23 January 2013)

We study a supersymmetric version of the type-III seesaw mechanism considering two variants of the model: a minimal version for explaining neutrino data with only two copies of **24** superfields and a model with three generations of **24**-plets. The latter predicts, in general, rates for $\mu \to e\gamma$ inconsistent with experimental data. However, this bound can be evaded if certain special conditions within the neutrino sector are fulfilled. In the case of two **24**-plets, lepton flavor violation constraints can be satisfied much more easily. After specifying the corresponding regions in the minimal supergravity parameter space, we show that under favorable conditions one can test the corresponding flavor structures in the leptonic sector at the LHC. For this we perform Monte Carlo studies for the signals, also taking into account the supersymmetry background. We find that it is only of minor importance for the scenarios studied here.

DOI: 10.1103/PhysRevD.87.013010 PACS numbers: 14.60.Pq, 12.60.Jv

I. INTRODUCTION

Neutrino oscillation experiments currently give the main indication for physics beyond the Standard Model. The observed tiny neutrino masses can be easily explained by the seesaw mechanism, which at tree level can be written in just three different variants [1], classified according to the $SU(2) \times U(1)$ representation of the postulated heavy particles: type I postulates fermionic gauge singlets [2–5]; type II, scalar $SU(2)$ triplets with hypercharge 1 [6,7]; and type III, fermionic triplets in the adjoint representation of $SU(2)$ [8]. At low energies they all lead to a unique dimension-5 operator [9,10]

$$(m^{\nu})_{\alpha\beta} = \frac{f_{\alpha\beta}}{\Lambda}(HL)(HL). \tag{1}$$

Neutrino experiments determine only $f_{\alpha\beta}/\Lambda$, but contain no information about the origin of this operator, nor about the absolute size of Λ. If f is a coefficient $\mathcal{O}(1)$, current neutrino data indicate $\Lambda \lesssim \mathcal{O}(10^{15})$ GeV. This value is close to, but slightly below, the scale of hypothetical grand unified theory (GUT), which should be larger than roughly 10^{16} GeV to avoid bounds from the nonobservation of proton decay.

A possible way to stabilize the large hierarchy between the GUT scale and the electroweak scale is with supersymmetry [11]. In its minimal form supersymmetry leads to a unification of the gauge couplings, in contrast to the SM [12–18]. Moreover, it can explain electroweak symmetry breaking as a radiative effect [19]. Supersymmetric variants of the different seesaw models have been considered by several authors; see e.g., Refs. [20–25]. In these models renormalization group evolution induces nonzero flavor mixing elements in the mass parameters of the sleptons even if they are flavor diagonal at the GUT scale. These off-diagonal elements in turn lead to sizable contributions to lepton flavor violating (LFV) observables [26]. In the case of the type-I seesaw mechanism, low-energy LFV decays such as $l_i \to l_j + \gamma$ and $l_i \to 3l_j$ have been calculated in Refs. [27–36]; $\mu - e$ conversion in nuclei has been studied in Refs. [37,38].

To maintain gauge coupling unification the seesaw particles need to be included in complete $SU(5)$ representations; i.e., one needs a **15**-plet in the case of type-II models and at least two **24**-plets in the case of type-III models. If one were to use only one **24**-plet, then one would need either nonrenormalizable operators at the GUT scale [39] or an extended $SU(5)$ Higgs sector [40] to explain neutrino data. The type-II and type-III models have received less attention than type-I models. Note, however, that the former actually has fewer free parameters than type-I models, implying that ratios of LFV decays of leptons can actually be predicted as a function of neutrino angles in minimal supergravity (mSUGRA) as discussed in Refs. [21,23]. For type-III models it has been shown in Ref. [25] that a generic model with three **24**-plets is heavily constrained by

*mahirsch@ific.uv.es
†porod@physik.uni-wuerzburg.de
‡Christof.Weiss@physik.uni-wuerzburg.de
§fnstaub@th.physik.uni-bonn.de

the bounds on rare lepton decays, in particular, due to the stringent bound on $\mu \to e\gamma$. The impact on $\mu \to e\gamma$ in a gauge mediated supersymmetry breaking embedding of type III was studied in Ref. [41], while in Ref. [42] possible LHC phenomenology from lepton-flavor violation was also discussed for the mSUGRA case.

In this paper we are first going to show under which conditions the type-III model is consistent with the experimental data. This will then be compared with a two-generation model where the bounds due to $\mu \to e\gamma$ are less stringent. Finally, we will address the following question: To what extent does the LHC observe lepton flavor violating processes in supersymmetric (SUSY) cascade decays. Compared to the previous study in Ref. [42] we do not only consider the case of two and three generations of **24**-plets, but we also take into account the recently measured reactor angle θ_{13}. Moreover, we demonstrate, in a Monte Carlo study for the LHC signal, that the SUSY background is well under control.

For the particle content we will assume the minimal supersymmetric standard model (MSSM) as framework. The recent observation of a Higgs-like state at the LHC with a mass around 125 GeV [43,44] can hardly be explained within GUT models with universal boundary conditions [45,46]. The same holds in variants including seesaw states at high scales [47]. However, it is well known that the singlet extension of the MSSM can more easily explain a Higgs mass of this size, as there are additional F-term contributions already at tree level (see e.g., Refs. [48–50] and references therein). Including an additional singlet does not lead to any significant changes in the slepton sector, as the singlet Yukawa couplings enter only at two-loop level in the renormalization group equations (RGEs) of the corresponding parameters. For this reason we do consider bounds from direct searches at the LHC but do not take into account the requirement of correctly explaining a Higgs mass of 125 GeV. To explain this condition and take into account the theoretical as well as experimental uncertainty, it would be sufficient to shift the tree-level Higgs mass for all points in the following by about 5 GeV. In the next-to-minimal supersymmetric Standard Model the tree-level mass of the light Higgs is given by [51]

$$m_Z^2\left(\cos^2 2\beta + \frac{\lambda^2}{g^2}\sin^2 2\beta\right), \tag{2}$$

where we introduced the superpotential coupling λ of the singlet to the Higgs doublets. Thus, assuming $\tan\beta = 10$ one would need $\lambda \simeq 0.6$, i.e., not too close to the perturbativity bound of 0.75. However, the exact value of $\tan\beta$ plays only a subdominant role for our analysis in the following. If we choose $\tan\beta = 5$, already $\lambda = 0.45$ would be sufficient. Since the singlino couples only very weakly to the sleptons, its role is negligible as long as it is not the lightest supersymmetric particle (LSP). However, it can only be the LSP if the trilinear self-coupling κ of the singlet field is much smaller than λ [52]. For example, in the scale invariant next-to-minimal supersymmetric Standard Model a bino LSP is a common feature [53]. Moreover, this constraint can easily be satisfied in more general singlet extensions with an explicit bilinear singlet term in the superpotential [54,55].

This paper is organized as follows: In the next section we summarize the main features of the two variants of the type-III model. In Sec. III we first discuss how to accommodate the rare lepton decays in type-III seesaw models. Afterwards we discuss lepton flavor violating signals from SUSY cascade decays and present the results of a Monte Carlo study. Finally, we draw our conclusions in Sec. IV.

II. MODELS AND SPECTRA

In this section we briefly summarize the main features of the supersymmetric version of the seesaw type-III model. In order to maintain gauge coupling unification for the type-III model, we add at the seesaw scale(s) additional particles to obtain a complete $SU(5)$ representation, i.e., a 24-plet. Note that the 24-plet actually also includes a gauge singlet and, thus, one always has a combination of the type-I and the type-III seesaws in this model.

In the subsequent sections we present the superpotentials and the relation of the parameters to neutrino physics. In addition, there are corresponding soft SUSY breaking terms which, however, reduce at the electroweak scale to the MSSM ones and, thus, are not discussed further. There are additional terms of the soft SUSY breaking potential, due to the heavy particles, that we do not discuss either, as their effect is, at most, of the order $M_{\rm EWSB}/M_{\rm seesaw}$ and, thus, can be safely neglected.

In this paper we will assume common soft SUSY breaking parameters at the GUT scale $M_{\rm GUT}$ to specify the spectrum at the electroweak scale: a common universal gaugino mass $M_{1/2}$, a common scalar mass m_0, and the trilinear coupling A_0, which gets multiplied by the corresponding Yukawa couplings to obtain the trilinear couplings in the soft SUSY breaking Lagrangian. In addition, the sign of the μ parameter is fixed, as is $\tan\beta = v_u/v_d$ (at the electroweak scale), where v_d and v_u are the the vacuum expectation values (vevs) of the neutral component of H_d and H_u, respectively. The models discussed below also contain new bilinear parameters in the superpotential, leading to additional bilinear terms in the soft SUSY breaking potential which are proportional to B_0 of the MSSM Higgs sector. The corresponding RGEs decouple, and their only effect is a small mass splitting between the new heavy scalar particles from the new heavy fermionic states of the order $B_0/M_{\rm seesaw}$. This leads to a tiny effect in the calculation of the thresholds at the seesaw scale(s) [56] which, however, we can safely neglect.

A. Supersymmetric type-III seesaw model

In the case of a type-III seesaw model one needs new fermions Σ at the high scale belonging to the adjoint

representation of $SU(2)$. This has to be embedded in a **24**-plet to obtain a complete $SU(5)$ representation. The superpotential of the unbroken $SU(5)$ relevant for our discussion is

$$W = \sqrt{2}\bar{5}_M Y^5 10_M \bar{5}_H - \frac{1}{4} 10_M Y^{10} 10_M 5_H + 5_H 24_M Y_N^{\mathrm{III}} \bar{5}_M + \frac{1}{2} 24_M M_{24} 24_M. \quad (3)$$

Here we have not specified the Higgs sector responsible for the $SU(5)$ breaking as it only enters logarithmically via threshold corrections at the GUT scale and, thus, plays a minor role for the subsequent discussion. The new parts, which will give the seesaw mechanism, come from the 24_M. It decomposes under $SU(3) \times SU(2) \times U(1)$ as

$$\begin{aligned} 24_M &= (1,1,0) + (8,1,0) + (1,3,0) \\ &\quad + (3,2,-5/6) + (3^*,2,5/6), \\ &= \hat{B}_M + \hat{G}_M + \hat{W}_M + \hat{X}_M + \hat{\bar{X}}_M. \end{aligned} \quad (4)$$

The fermionic components of (1, 1, 0) and (1, 3, 0) have exactly the same quantum numbers as a right-handed neutrino ν^c and the required $SU(2)$ triplet Σ. Thus, the 24_M always produces a combination of the type-I and type-III seesaws.

In the $SU(5)$ broken phase the superpotential becomes

$$\begin{aligned} W_{\mathrm{III}} &= W_{\mathrm{MSSM}} + \hat{H}_u \left(\hat{W}_M Y_N - \sqrt{\frac{3}{10}} \hat{B}_M Y_B \right) \hat{L} \\ &\quad + \hat{H}_u \hat{\bar{X}}_M Y_X \hat{D}^c + \frac{1}{2} \hat{B}_M M_B \hat{B}_M + \frac{1}{2} \hat{G}_M M_G \hat{G}_M \\ &\quad + \frac{1}{2} \hat{W}_M M_W \hat{W}_M + \hat{X}_M M_X \hat{\bar{X}}_M. \end{aligned} \quad (5)$$

As before, we use at the GUT scale the boundary conditions $Y_N = Y_B = Y_X$ and $M_B = M_G = M_W = M_X$. Y_N, Y_B and Y_X are $n \times 3$ matrices, while M_G, M_W and M_X are $n \times n$-dimensional matrices if we include n generations of 24-plets. Integrating out the heavy fields yields the following formula for the neutrino masses at the low scale:

$$m_\nu = -\frac{v_u^2}{2} \left(\frac{3}{10} Y_B^T M_B^{-1} Y_B + \frac{1}{2} Y_W^T M_W^{-1} Y_W \right). \quad (6)$$

As mentioned above there are two contributions—one from the gauge singlet, the other from the $SU(2)$ triplet. In this case the calculation of the Yukawa couplings in terms of a given high scale spectrum is more complicated than in the other two types of seesaw models. However, as we start from universal couplings and masses at M_{GUT} we find that at the seesaw scale one still has $M_B \simeq M_W$ and $Y_B \simeq Y_W$, so one can write to a good approximation

$$m_\nu = -v_u^2 \frac{4}{10} Y_W^T M_W^{-1} Y_W. \quad (7)$$

Being complex symmetric, the light Majorana neutrino mass matrix in Eq. (7) is diagonalized by a unitary 3×3 matrix U [6],

$$\hat{m}_\nu = U^T \cdot m_\nu \cdot U. \quad (8)$$

Inverting the seesaw equation (7) allows us to express Y_W as [57]

$$Y_W = \frac{i 4\sqrt{2}}{5 v_u} \sqrt{\hat{W}_M} \cdot R \cdot \sqrt{\hat{m}_\nu} \cdot U^\dagger, \quad (9)$$

for $n = 3$, where the $\hat{m}_\nu$ and $\hat{W}_M$ are diagonal matrices containing the corresponding eigenvalues. R is, in general, a complex orthogonal matrix which is characterized by three angles ϕ_i which are, in general, complex. Note that, in the special case $R = \mathbf{1}$, Y_W contains only "diagonal" products $\sqrt{M_i m_i}$. For U we will use the standard form

$$U = \begin{pmatrix} c_{12}c_{13} & s_{12}c_{13} & s_{13}e^{-i\delta} \\ -s_{12}c_{23} - c_{12}s_{23}s_{13}e^{i\delta} & c_{12}c_{23} - s_{12}s_{23}s_{13}e^{i\delta} & s_{23}c_{13} \\ s_{12}s_{23} - c_{12}c_{23}s_{13}e^{i\delta} & -c_{12}s_{23} - s_{12}c_{23}s_{13}e^{i\delta} & c_{23}c_{13} \end{pmatrix} \times \begin{pmatrix} e^{i\alpha_1/2} & 0 & 0 \\ 0 & e^{i\alpha_2/2} & 0 \\ 0 & 0 & 1 \end{pmatrix} \quad (10)$$

with $c_{ij} = \cos(\theta_{ij})$ and $s_{ij} = \sin(\theta_{ij})$. The angles θ_{12}, θ_{13} and θ_{23} are the solar neutrino angle, the reactor (or CHOOZ) angle and the atmospheric neutrino mixing angle, respectively. δ is the Dirac phase and α_i are Majorana phases. In the following we will set the latter to 0 and consider for δ mainly the cases 0 and π.

B. Supersymmetric type-III seesaw model with two 24-plets

Current neutrino experiments only determine the differences of the neutrino masses squared. Thus it might well be that only two of the light neutrinos are massive, whereas the third is either massless or has a mass much smaller than the others. Such a situation is obtained if only two **24**-plets are present, similarly to the case of the type-I seesaw model with two right-handed neutrinos as discussed for example in Refs. [58–60]. We call this class of models 3×2 seesaw models (see also Ref. [61]).

In the following we work in the basis where M_W is a 2×2 diagonal matrix, denoting the eigenvalues by $\hat{M}_i$ ($i = 1, 2$). Similarly to the three-generation case one can express the Y_W in terms of a low-energy neutrino parameter

and model-dependent high-energy parameters, as also discussed in the context of seesaw I models [62]:

$$Y_W = \sqrt{\frac{5}{2}}\frac{i}{v_u}\sqrt{M_W}R\left(\sqrt{\hat{m}_\nu^{-1}}\right)' U^\dagger. \tag{11}$$

The R matrix is now a 2×3 matrix which can assume the following forms:

$$R_{\text{norm}} = \begin{pmatrix} 0 & \cos(\phi) & -\sin(\phi) \\ 0 & \sin(\phi) & \cos(\phi) \end{pmatrix} \tag{12}$$

in the case of normal hierarchy in the neutrino sector ($m_1 = 0$), and for inverse hierarchy ($m_3 = 0$),

$$R_{\text{norm}} = \begin{pmatrix} \cos(\phi) & -\sin(\phi) & 0 \\ \sin(\phi) & \cos(\phi) & 0 \end{pmatrix}. \tag{13}$$

Note that the R matrix is parametrized by one complex angle ϕ only, in contrast to the three-generation case.

C. Lepton flavor violation in the slepton sector

From a one-step integration of the RGEs one gets, assuming mSUGRA boundary conditions, a first rough estimate for the lepton flavor violating entries in the slepton mass parameters:

$$(\Delta m_L^2)_{ij} \simeq -\frac{a_k}{8\pi^2}(3m_0^2 + A_0^2)(Y_W^{k,\dagger} L Y_W^k)_{ij}, \tag{14}$$

$$(\Delta A)_{l,ij} \simeq -a_k \frac{3}{16\pi^2} A_0 (Y_e Y_W^{k,\dagger} L Y_W^k)_{ij}, \tag{15}$$

for $i \neq j$ in the basis where Y_e is diagonal, $L_{ij} = \ln(M_{\text{GUT}}/M_i)\delta_{ij}$ and Y_W^k is the additional Yukawa coupling where k indicates the number of **24**-plets,

$$a_2 = \frac{6}{5} \quad \text{and} \quad a_3 = \frac{9}{5}. \tag{16}$$

Both models have in common that they predict negligible flavor violation for the right sleptons,

$$(\Delta m_E^2)_{ij} \simeq 0, \tag{17}$$

which is a general feature of the usual seesaw models [25]. Although it is known that approximations (14) and (15) do not reproduce well the actual size of the off-diagonal elements, they do give the functional dependencies on the high scale parameters. Therefore, they are a useful indicator of how the rare lepton decays $l_i \to l_j \gamma$ depend on these parameters, as the corresponding decay modes scale roughly like

$$\text{Br}(l_i \to l_j \gamma) \propto \alpha^3 m_{l_i}^5 \frac{|(\Delta m_L^2)_{ij}|^2}{\tilde{m}^8} \tan^2\beta, \tag{18}$$

where $\tilde{m}$ is the average of the SUSY masses involved in the loops. Using the parametrization for the Yukawa couplings of Eq. (9), the entries in $(\Delta m_L^2)_{ij}$ can be expressed as

$$(\Delta m_L^2)_{ij} \propto U_{i\alpha} U_{j\beta}^* \sqrt{m_\alpha}\sqrt{m_\beta} R_{k\alpha}^* R_{k\beta} M_k \log\left(\frac{M_X}{M_k}\right). \tag{19}$$

In the special case where the matrix R is the identity matrix, Eq. (19) reduces to

$$\begin{aligned}
(\Delta m_L^2)_{12} &\propto c_{12}c_{13}(-s_{12}c_{23} - c_{12}s_{23}s_{13}e^{-i\delta})z_1 + s_{12}c_{13}(c_{12}c_{23} - s_{12}s_{23}s_{13}e^{-i\delta})z_2 + s_{23}c_{13}s_{13}e^{-i\delta}z_3 \\
(\Delta m_L^2)_{13} &\propto c_{12}c_{13}(s_{12}s_{23} - c_{12}c_{23}s_{13}e^{-i\delta})z_1 + s_{12}c_{13}(-c_{12}s_{23} - s_{12}c_{23}s_{13}e^{-i\delta})z_2 + c_{23}c_{13}s_{13}e^{-i\delta}z_3 \\
(\Delta m_L^2)_{23} &\propto (s_{12}s_{23} - c_{12}c_{23}s_{13}e^{-i\delta})(-s_{12}c_{23} - c_{12}s_{23}s_{13}e^{i\delta})z_1 \\
&\quad + (-c_{12}s_{23} - s_{12}c_{23}s_{13}e^{-i\delta})(c_{12}c_{23} - s_{12}s_{23}s_{13}e^{i\delta})z_2 + s_{23}c_{23}c_{13}^2 z_3,
\end{aligned} \tag{20}$$

where

$$z_i \equiv m_i M_i \log\left(\frac{M_X}{M_i}\right). \tag{21}$$

For the ansatz of degenerate seesaw states the combination $M_i \log(\frac{M_X}{M_i})$ becomes an overall factor; i.e., for degenerate $M_B = M_W$ one may simply make the replacement $z_i \to m_i$ in Eq. (20). For strict normal hierarchy, the expressions become even simpler. For instance, Δm_L^2 becomes

$$\begin{aligned}
(\Delta m_L^2)_{12} \propto \Big(& s_{13}s_{23}\sqrt{\Delta(m_{\text{Atm}}^2) + \Delta(m_\odot^2)} - \sqrt{\Delta(m_\odot^2)}s_{12}^2 \\
& + c_{12}c_{23}e^{i\delta}\sqrt{\Delta(m_\odot^2)}s_{12}\Big).
\end{aligned} \tag{22}$$

Inserting the best-fit point data for oscillation parameters, except for s_{13}, and assuming $\delta = \pi$ one can calculate the value for s_{13}^2 for which Δm_L^2 approximately vanishes as $s_{13}^2 = 0.0077$, which agrees very well with the full numerical calculation shown in the next section (see Fig. 2).

Similar analytical estimates can be calculated in other limits and, even though absolute values for LFV processes are only rough estimates, ratios of LVF quantities can be calculated quite accurately in this way.

In numerical studies we will use the complete formulas as given in Refs. [32,63]. We will also consider the three-body decays $\text{BR}(l_i \to 3l_j)$ where we use the formulas given in Ref. [32].

III. NUMERICAL RESULTS

In this section we present our numerical calculations. All results presented below have been obtained with the lepton flavor violating version of the program package SPheno [64,65]. The RGEs of the two seesaw III models have been calculated with SARAH [66–69]. For the Monte Carlo studies below we have used the SUSY TOOLBOX [70] to generate the interface to WHIZARD [71].

All seesaw parameters as well as the soft SUSY breaking parameters are defined at $M_{\rm GUT}$. We evolve the RGEs to the scales corresponding to the GUT-scale values of the masses of the heavy particles. The RGE evolution also implies a splitting of the heavy masses up to 20% between the gauge singlet and the color octet. We therefore add, at the corresponding scale, the threshold effects due to the heavy particles to account for the different masses as discussed in Ref. [25]. However, since the gauge singlet does not contribute to the running of the gauge couplings, the main impact on gauge coupling unification is due to mass splitting between the color octet and the $SU(2)_L$ triplet. This splitting is for a seesaw scale of $O(10^{14}$ GeV) of the order of 10% and would result in a marginal shift of $O(10^{-4})$ for the gauge couplings. Off-diagonal elements are induced in the mass matrices of the **24**-plets. This implies that one has to go to the corresponding mass eigenbasis before calculating the threshold effects. We use two-loop RGEs everywhere.

Unless mentioned otherwise, we fit neutrino mass squared differences to their best-fit values [72]. Our numerical procedure is as follows: Inverting the seesaw equation [see Eqs. (9) and (11)], one can get a first guess for the Yukawa couplings for any fixed values of the light neutrino masses (and angles) as a function of the corresponding triplet mass for any fixed value of the couplings. This first guess will not give the correct Yukawa couplings, since the neutrino masses and mixing angles are measured at low energy, whereas for the calculation of m_ν we need to insert the parameters at the high-energy scale. However, it can be used to numerically run the RGEs to obtain the exact neutrino masses and angles (at low energies) for these input parameters. The difference between the results obtained numerically and the input numbers can then be minimized in a simple iterative procedure until convergence is achieved. As long as neutrino Yukawas are $|Y_{W,ij}| < 1\ \forall i, j$ we reach convergence in a few steps.

A. Bounds from lepton decays

It has been known for some time that generically the supersymmetric seesaw III model predicts rates for $\mu \to e\gamma$ which are too large [25] to be compatible with the experimental bound for $\mathrm{BR}(\mu \to e\gamma) \lesssim 2.4 \times 10^{-12}$ [73]. However, this does not completely exclude the model, as there are certain parameter regions where cancellations between different contributions can occur. In this section we explore the different possibilities. For the corresponding regions the question arises as to whether they can be probed by other experiments, in particular, the LHC. From the discussion in the previous section, in particular, Eqs. (14) and (18), the rare leptons decays are mainly governed by the overall SUSY mass scale and the lepton flavor entries. The LFV entries in the soft breaking terms are nearly completely governed by the choice of parameters in the heavy seesaw sector, while the dependence on the soft SUSY parameters is much weaker. We therefore fix the latter to

$$m_0 = 1000\ \text{GeV}, \qquad M_{1/2} = 1000\ \text{GeV}, \qquad A_0 = 0 \quad \text{and} \quad \mu > 0. \tag{23}$$

In Fig. 1 we recall the generic situation for the type-III seesaw model. The dashed and solid lines correspond to the two- and three-generation models, respectively. Only a certain range for $M_{\rm Seesaw}$ is allowed. The lower bounds stem from the fact that the gauge couplings become nonperturbative at the GUT scale, whereas the upper bounds are due to nonperturbative Yukawa couplings at the GUT scale [25]. Every **24**-plet contributes with $\Delta b_i = 5$ to the beta functions of the gauge couplings g_i and, thus, obviously the possible range is larger for the two-generation case compared to the three-generation case.

Equations (9) and (11) imply that one can induce special features for the Yukawa couplings when varying $\sin\theta_{13}$, the CP and/or elements of the R matrix, as has also been noted in Ref. [34] in the case of supersymmetric seesaw I models. This has an immediate impact on the flavor mixing entries of the slepton mass parameters, as can be seen from Eqs. (14) and (15). As an example we show in Fig. 2 the dependence on θ_{13} in the range allowed before the results of Daya Bay [74] and RENO [75], assuming three different values for the Dirac phase δ and a degenerate mass of 10^{14} GeV for the **24**-plets. Note that in this particular case the elements of the R matrix do not play any role. As can be

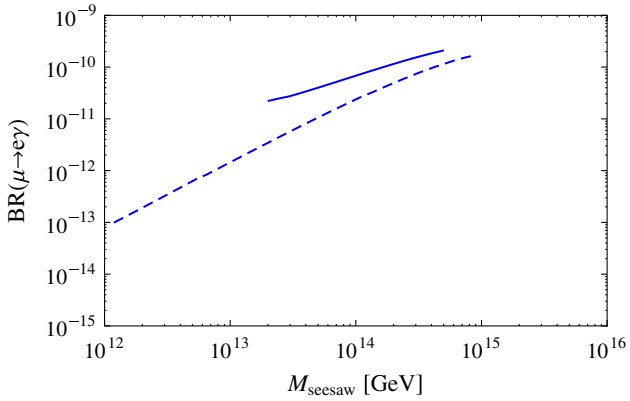

FIG. 1 (color online). $\mathrm{BR}(\mu \to e\gamma)$ versus the seesaw scale for the two (dashed) and the three (solid) **24**-plet scenarios. The mSUGRA parameters of Eq. (23) have been used, neutrino data was fixed to the current experimental values, including $\sin^2\theta_{13} = 0.026$.

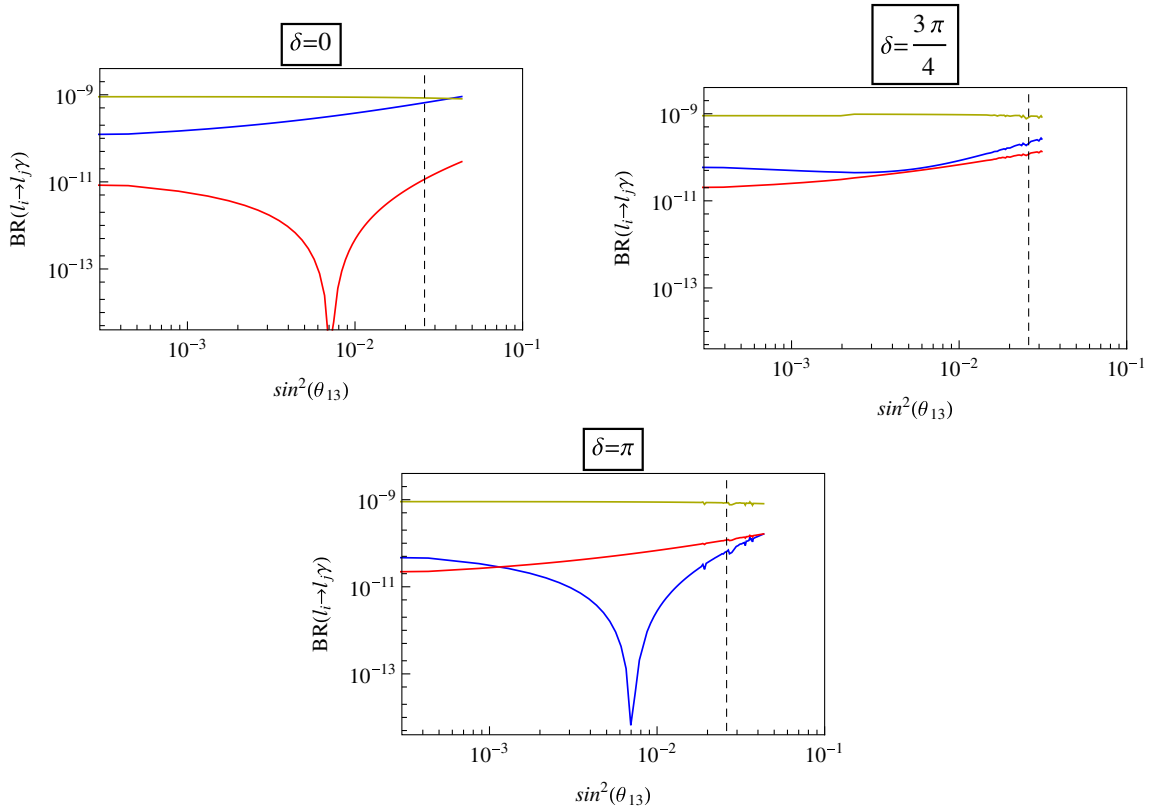

FIG. 2 (color online). BR($\mu \to e\gamma$) (blue/black line), BR($\tau \to e\gamma$) (red/dark gray line) and BR($\tau \to \mu\gamma$) (yellow/light gray line) over the reactor angle θ_{13} for real parameters with Dirac phases $\delta = 0$ (upper left), $\delta = \pi$ (upper right) and $\delta = 3\pi/4$ (lower panel). We set $M_W = 10^{14} \cdot \mathbb{1}_3$ and the SUSY parameters as in Eq. (23). The dashed line indicates the current best-fit value for θ_{13}.

seen, δ has to be close to π in this case to get BR($\mu \to e\gamma$) below the experimental bound. For completeness we note that the small spikes in the plots are numerical artifacts of our iterations procedure.

With the recent measurement of θ_{13} by Daya Bay and RENO one can now relate seesaw parameters from the requirement to respect the bound on $\mu \to e\gamma$.[1] As an example we fix in Fig. 3 $\delta = \pi$, $\hat{M}_1 = \hat{M}_2 = 10^{14}$ GeV and take $R = \mathbb{1}_3$. In this case the bound on $\mu \to e\gamma$ is satisfied if $\hat{M}_3$ is close to 5×10^{13} GeV. Note, however, that the numbers obtained depend on the SUSY point chosen in parameter space. Therefore, one can start to constrain the seesaw parameters only after the discovery and subsequent determination of the SUSY parameters. In Fig. 4 we show a similar graph but for the two-generation model. The interesting point is that despite fewer parameters one still has sufficient freedom to suppress the rare lepton decays. On the one hand, this shows the need to determine not only the differences of the neutrino masses squared but also the absolute neutrino mass scale or, in other words, the mass of the lightest neutrino, as a nonzero value of the latter would rule out the minimal two-generation model or require its extension by nonrenormalizable operators. On the other hand, it implies that for the exploration of the LHC phenomenology it is sufficient to study the simpler two-generation model.

Up to now we have assumed that the R matrix is the unit matrix. In Fig. 5 we study the dependence on the R matrix in the two-generation model. We fix the **24**-plet masses to 5×10^{13} GeV and 5×10^{14} GeV and vary $\sin(\phi)$.

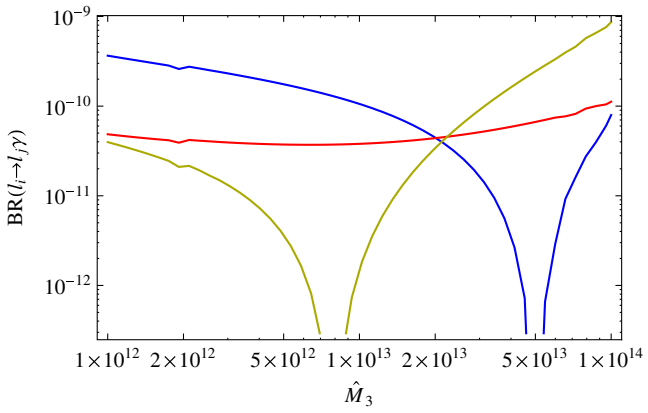

FIG. 3 (color online). BR($\mu \to e\gamma$) (blue/black line), BR($\tau \to e\gamma$) (red/dark gray line) and BR($\tau \to \mu\gamma$) (yellow/light gray line) as functions of $\hat{M}_3$ with θ_{13} at the current best-fit value. We have taken $\delta = \pi$, $\hat{M}_1 = \hat{M}_2 = 10^{14}$ GeV and the other parameters as in Eq. (23).

[1]For a recent update on $\mu \to e\gamma$ in seesaw type-I models taking into account the measured value of θ_{13}, see Ref. [76].

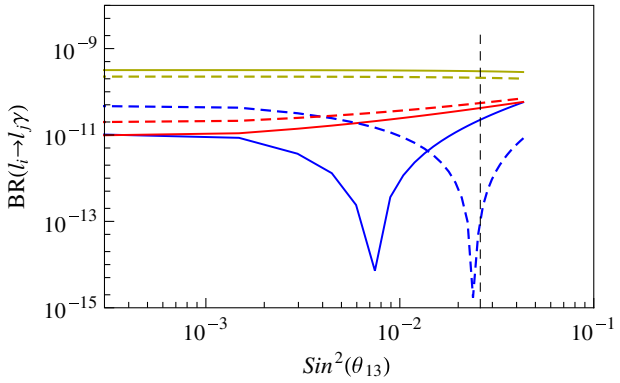

FIG. 4 (color online). BR($\mu \to e\gamma$) (blue/black line), BR($\tau \to e\gamma$) (red/dark gray line) and BR($\tau \to \mu\gamma$) (yellow/light gray line) as functions of $\sin^2\theta_{13}$ in the two-generation model for $\delta = \pi$, $\hat{M}_1 = \hat{M}_2 = 10^{14}$ GeV (solid lines) and $\hat{M}_1 = 2\times 10^{14}$ GeV, $\hat{M}_2 = 10^{14}$ GeV (dashed lines). The other parameters are as in Eq. (23).

Note that in both cases we have taken $\cos\phi > 0$. Instead of taking $\hat{M}_1 > \hat{M}_2$ we could have taken $\cos\phi < 0$ in the second plot. As expected, we find that variation of the R matrix provides additional possibilities to suppress BR($\mu \to e\gamma$) below the current experimental bound. Moreover, our results show that one can never exclude this class of models by these measurements, as with a sufficient tuning of parameters one can always avoid the bounds.

For completeness we compare in Fig. 6 the branching ratios of the two-body decays $l_i \to l_j\gamma$ to the ones for the three-body decays $l_i \to 3l_j$ in the three-generation model. Similar to the seesaw type-I case [32] we see that both decay classes show the same dependence on the underlying parameters, since in the case of the three-body decays the photon contribution dominates. We have checked that this also holds for the two-generation model.

B. Testing flavor structures at the LHC

We have seen in the previous section that one can choose the seesaw parameters such that the experimental constraints on the rare lepton decays are fulfilled. In this section we address the question of whether there are any possibilities to test these models for such parameter choices at the LHC. As we will demonstrate there are indeed favorable SUSY parameter regions where one can observe the corresponding flavor violating decays of supersymmetric particles.

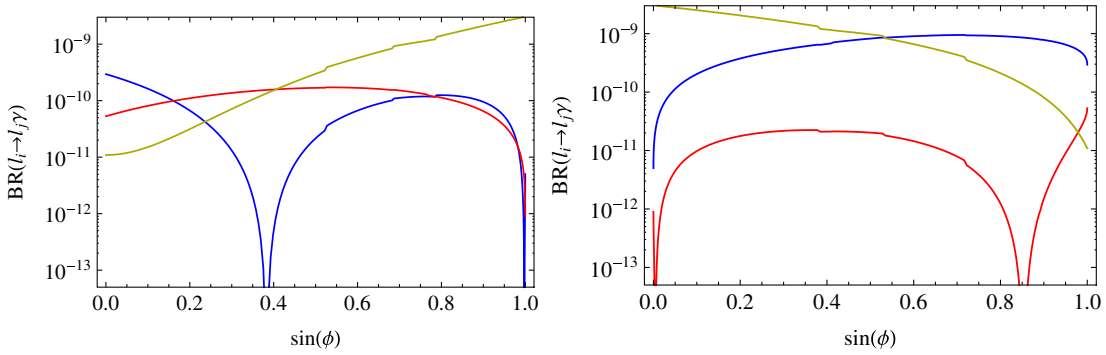

FIG. 5 (color online). BR($\mu \to e\gamma$) (blue/black line), BR($\tau \to e\gamma$) (red/dark gray line) and BR($\tau \to \mu\gamma$) (yellow/light gray line) as functions of $\sin\phi$ for two **24**-plets with masses $\hat{M}_1 = 5\times 10^{14}$ GeV and $\hat{M}_2 = 5\times 10^{13}$ GeV on the left panel (right panel—vice versa, $\hat{M}_1 > \hat{M}_2$), $\delta = 0$ and the SUSY parameters as in Eq. (23).

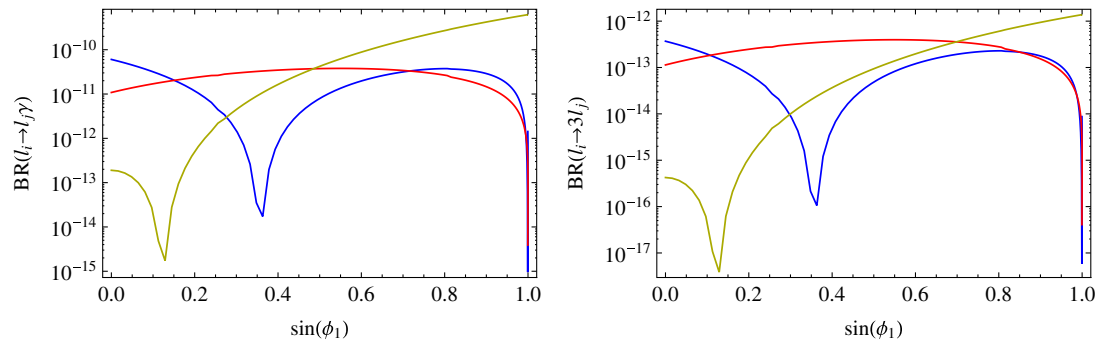

FIG. 6 (color online). Comparison of the two-body decays $l_i \to l_j\gamma$ (left panel) and the three-body decays $l_i \to 3l_j$ (right panel) for variation of $\sin(\phi_1)$ at normal neutrino mass hierarchy, Dirac phase $\delta = 0$ and a **24**-plet hierarchy: $\hat{M}_1 = 10^{15}$ GeV, $\hat{M}_2 = 10^{14}$ GeV and $\hat{M}_3 = 10^{13}$ GeV; l_i, $l_j = \mu$, e (blue/black line); τ, e (red/dark gray line); τ, μ (yellow/light gray line).

The branching ratios of the lepton flavor violating decays of sleptons and neutralinos are governed by the same entries in the slepton mass matrix as the rare lepton decays, i.e., the ones given in Eqs. (14) and (15). Therefore, both classes of decays show the same dependence on the seesaw parameters.

At the LHC one has to study cascade decays containing sequences of the form $\tilde{\chi}_2^0 \to \tilde{l}_k^{\mp} l_j^{\mp} \to l_i^{\pm} l_j^{\mp} \tilde{\chi}_1^0$ with $i \neq j$ [36,77–83]. Moreover, the nature of the neutralinos should be dominantly gaugino-like and the mass difference should be small enough to suppress the decay into h^0. This requires a certain hierarchy between the neutralino mass parameters and the slepton mass parameters which is roughly given by $|\mu| \gg M_2 \gtrsim m_{\tilde{l}} \gtrsim M_1$ where the ordering of M_1 and M_2 can be interchanged.

As the scaling of the lepton flavor violating decays of SUSY particles is similar to the one of the rare lepton decays in this class of models, we use the following strategy to enhance the rates for $\tilde{\chi}_2^0 \to \tilde{e}^{\pm}\mu^{\mp}\chi_1^0$, $\tilde{\chi}_2^0 \to \tilde{e}^{\pm}\tau^{\mp}\chi_1^0$ and $\tilde{\chi}_2^0 \to \tilde{\mu}^{\pm}\tau^{\mp}\chi_1^0$. For a given point in the SUSY parameter space we choose the seesaw parameters in the following way: We fix the R matrix to be either $\mathbb{1}$ or as in Eq. (12), depending on whether we work in the two- or three-generation seesaw model. Next we fix the relative size of various entries of Y_W such that the neutrino mixing matrix is tribimaximal. Note that a nonzero θ_{13} changes the neutralino branching ratios only slightly and, thus, its effect can be neglected here. In the third step both Y_W and M_W are rescaled until the correct neutrino masses are obtained and 10^{12}. $\mathrm{BR}(\mu \to e\gamma)$ is in the interval [2.2, 2.4]. In this way one obtains the maximum rate for the decay $\tilde{\chi}_2^0 \to \tilde{e}^{\pm}\mu^{\mp}\chi_1^0$ which is the cleanest at the LHC [80,81]. With a further variation of the entries in Y_W one could increase the final states containing a τ lepton. However, we have checked for a couple of points in the SUSY parameter space that this would only lead to a relative increase of about 10% for the corresponding rates. We have not pursued this further, as this is at most of the order of the expected theoretical uncertainty on the SUSY cross section, which is about 10%–20% (see e.g., Refs. [84–87] and references therein). In the following examples we have checked that the bounds on SUSY particles are fulfilled [88–91].

The branching ratios of the lepton flavor violating decays can reach up to a few percent, as shown in Fig. 7. The structure of the RGEs implies that the three heaviest sleptons are essentially $\tilde{l}_L$, even though there can be sizable mixing between the stau states. The latter mixing is the main source of the LFV decays for $M_{1/2} \lesssim 1550$ GeV, where only the three lightest sleptons appear in the $\tilde{\chi}_2^0$ decays. The hierarchy $\mathrm{BR}(\tilde{\chi}_2^0 \to \tilde{\chi}_1^0\tau\mu) > \mathrm{BR}(\tilde{\chi}_2^0 \to \tilde{\chi}_1^0\mu e) > \mathrm{BR}(\tilde{\chi}_2^0 \to \tilde{\chi}_1^0\tau e)$ is a consequence of the structure of Y_W needed to explain the neutrino data. The change of the spectrum has two main sources: (i) $M_{1/2}$ enters the RGEs for the slepton mass parameters and (ii) the requirement that $\mathrm{BR}(\mu \to e\gamma)$ is in the above interval implies that the seesaw scale becomes a function of $M_{1/2}$. Changing the seesaw scale has a major impact on the spectrum, as discussed in detail in Ref. [25]. Similar features show up in the two-generation model, as exemplified in Fig. 8 where we show the LFV $\tilde{\chi}_2^0$ decay branching ratios as a function of A_0. In this model one can find LFV branching ratios of up to 10%. The main reason for this is the different kinematics for the same mSUGRA input because changing the number of seesaw particles implies changes in the RGEs of the slepton and gaugino mass parameters, as discussed above.

We concentrate in the following on the two-generation model, as here the signal is somewhat larger than in the three-generation model. At the LHC $\tilde{\chi}_2^0$ is mainly produced in the cascade decays of squarks and gluinos. In Fig. 9 we show $\sigma \times \mathrm{BR}$ as a function of $M_{1/2}$, fixing the other parameters for two values of m_0, $A_0 = 0$, $\tan\beta = 10$, $\mu > 0$ and $\sqrt{s} = 14$ TeV. In addition, we use $\hat{M}_1 = \hat{M}_2 = 2.5 \times 10^{13}$ GeV as well as $Y_{W,11} = Y_{W,12} = -Y_{W,13} = -5.252 \times 10^{-2}$, $Y_{W,21} = 0$ and $Y_{W,22} = Y_{W,23} = -1.547 \times 10^{-1}$. Here we have summed over all possibilities to

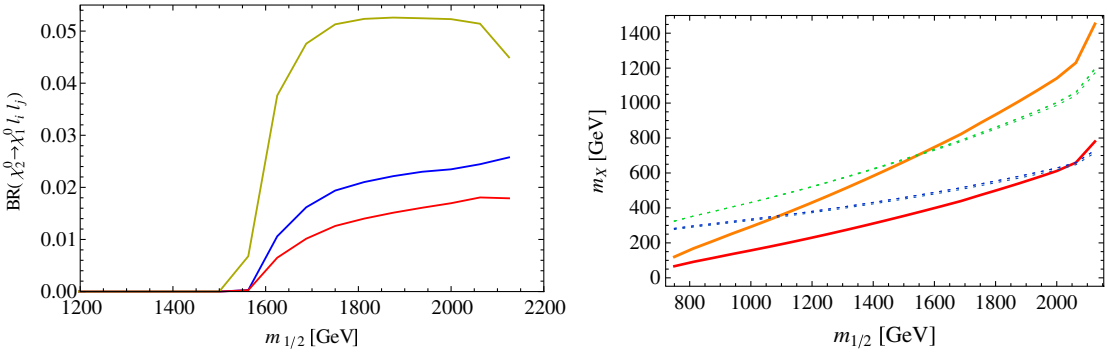

FIG. 7 (color online). $\mathrm{BR}(\tilde{\chi}_2^0 \to \tilde{\chi}_1^0 l_i l_j)$ and selected masses as a function of $M_{1/2}$ for $m_0 = 250$ GeV, $A_0 = 0$, $\tan\beta = 10$ and $\mu > 0$. Left plot: $\mathrm{BR}(\tilde{\chi}_2^0 \to \tilde{\chi}_1^0\mu e)$ (blue/black line), $\mathrm{BR}(\tilde{\chi}_2^0 \to \tilde{\chi}_1^0\tau e)$ (red/dark gray line) and $\mathrm{BR}(\tilde{\chi}_2^0 \to \tilde{\chi}_1^0\tau\mu)$ (yellow/light gray line); right plot: $\tilde{\chi}_2^0$ (orange/upper gray line), $\tilde{\chi}_1^0$ (red/lower gray line), $\tilde{l}_{1,2,3}$ (blue/gray dotted line) and $\tilde{l}_{4,5,6}$ (green/light gray dotted line). The neutrino parameters are at tribimaximal values, normal neutrino mass hierarchy and $R = \mathbb{1}$; M_W is varied to fit $\mathrm{BR}(\mu \to e\gamma)$ close to the experimental bound.

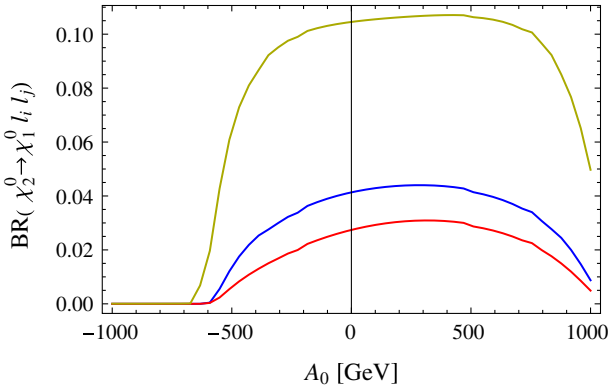

FIG. 8 (color online). BR($\tilde{\chi}_2^0 \to \tilde{\chi}_1^0 \mu e$) (blue/black line), BR($\tilde{\chi}_2^0 \to \tilde{\chi}_1^0 \tau e$) (red/dark gray line) and BR($\tilde{\chi}_2^0 \to \tilde{\chi}_1^0 \tau \mu$) (yellow/light gray line) in the two-generation model as functions of A_0 for $m_0 = 250$ GeV, $M_{1/2} = 1800$ GeV, $\tan\beta = 10$ and $\mu > 0$. The seesaw parameters are fixed as explained in the text.

produce squarks and gluinos, and we require that the two leptons from $\tilde{\chi}_2^0$ are the only ones in the event. For the calculation of the cross section we have used the LHC-FASER package [92,93]. One sees that the signal cross section before any cuts can be at most a few fb, which gives at most a few hundred events even for an integrated luminosity of 300 fb^{-1}.

This naturally leads to the question of whether such a signal can be observed at all. For this reason we have performed a Monte Carlo study at the parton level taking $m_0 = 50$ GeV, $M_{1/2} = 1484$ GeV, $A_0 = 0$, $\tan\beta = 10$ and $\mu > 0$, corresponding to a maximum of the signal in Fig. 9. For the generation of the events we use WHIZARD [71]. The corresponding signal cross sections are 1.4, 0.8 and 3.8 fb for the final states containing $e\mu$, $e\tau$ and $\mu\tau$, respectively. Related studies have been performed in Refs. [77,80,94], where it has been shown that one can

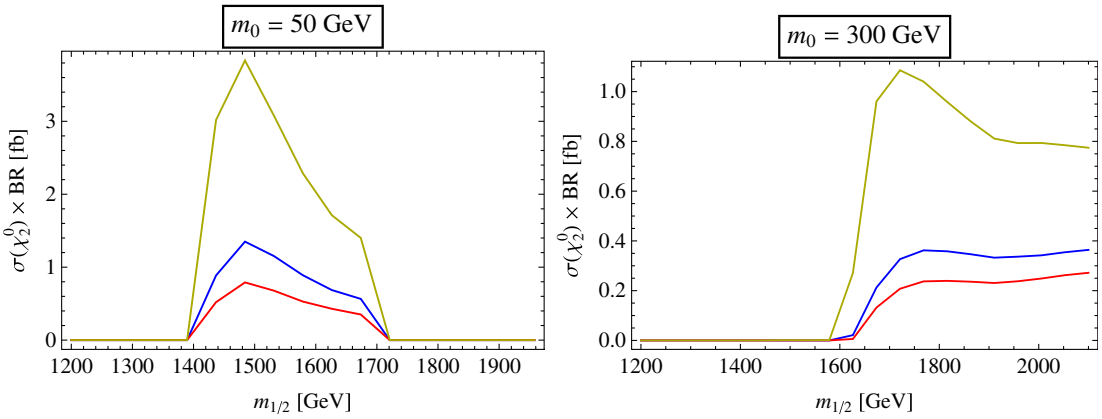

FIG. 9 (color online). Grid calculation of $\sigma(\tilde{\chi}_2^0) \times \text{BR}(\tilde{\chi}_2^0 \to \tilde{\chi}_1^0 \mu e)$ (blue/black line), $\sigma(\tilde{\chi}_2^0) \times \text{BR}(\tilde{\chi}_2^0 \to \tilde{\chi}_1^0 \tau e)$ (red/dark gray line) and $\sigma(\tilde{\chi}_2^0) \times \text{BR}(\tilde{\chi}_2^0 \to \tilde{\chi}_1^0 \tau \mu)$ (yellow/light gray line) in femtobarn over $M_{1/2}$ for different values of m_0; $A_0 = 0$, $\tan\beta = 10$ and $\mu > 0$. The seesaw parameters are fixed as explained in the text.

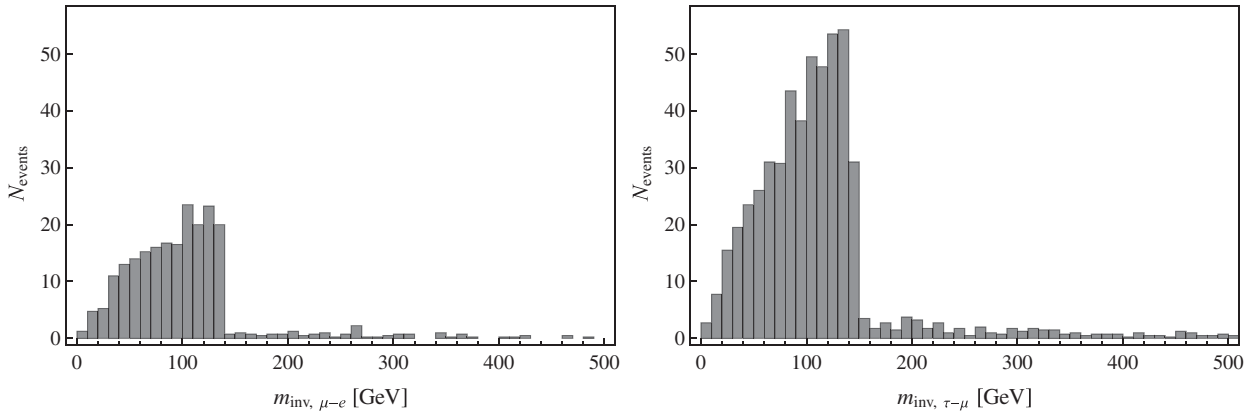

FIG. 10. Invariant mass distributions for the signal and SUSY background for final states containing μ, e (left plot) or τ, μ (right plot), missing transverse energy and at least two jets in the final state for a luminosity of 300 fb^{-1}, $m_0 = 50$ GeV, $M_{1/2} = 1484$ GeV, $A_0 = 0$, $\tan\beta = 10$ and $\mu > 0$.

reduce the SM background sufficiently. However, to our knowledge the SUSY background has not yet been taken into account. This will also be considered here. The main SM background is due to $t\bar{t}$, VV and Vjj ($V = W, Z$) production. In Ref. [95], where a detector study for the $\mu\tau$ channel has been performed for $\sqrt{s} = 10$ TeV, it has been shown that the SM background can be reduced significantly by requiring a cut on the missing transverse energy $\not{E}_T > 140$ GeV and a cut on the effective mass $M_{\rm eff} > 400$ GeV where

$$M_{\rm eff} \equiv \not{E}_T + \sum_{i=1}^{4} p_T^{\rm jet} + \sum_j p_T^l.$$

The first sum is over the transverse momentum of the four hardest jets and the second one is over the transverse momentum of all leptons. We have adjusted these cuts for the case $\sqrt{s} = 14$ TeV and use $\not{E}_T > 150 M_{\rm eff} > 1200$ GeV. Moreover, we require that the event contains exactly two leptons and no b jets. This reduces the SM background to a negligible level. The main SUSY background is due to charginos and W bosons produced in the SUSY cascade decays. In contrast to the signal these events stem, in general, from cascade decays of different squarks and/or gluinos. Therefore, if one plots the differential cross section as a function of the invariant lepton mass $m_{ll'} = \sqrt{(p_l + p_{l'})^2}$, one gets a triangle for the peak and a flat distribution from the background. We have simulated the combination of signal with SUSY background using the dominant production mechanism, which is in this case squark-squark production as the squarks are much lighter than the gluino, yielding about 80% of the total cross section. The results for an integrated luminosity of 300 fb^{-1} are shown in Fig. 10 where we have cut the range of $m_{ll'}$ at 500 GeV even though the SUSY background continues to be flat until about 1 TeV. As can be seen, one gets approximately the triangular shape of the signal with the edge at

$$m_{ll'}^2 = \frac{(m_{\tilde{\chi}_2^0}^2 - m_{\tilde{l}}^2)(m_{\tilde{l}}^2 - m_{\tilde{\chi}_2^0}^2)}{m_{\tilde{l}}^2}, \tag{24}$$

where the lepton masses have been neglected. The edge clearly indicates the consecutive two-body decays giving a first hint on the mass ordering. As the sleptons have different masses, they give somewhat different values for the edges which are collected in Table. I. Figure 10 clearly shows that in this case the SUSY background is negligible compared to the signal. Note that the light sleptons hardly contribute to the signal, as argued above, and, thus, the edges are essentially due to the heavier sleptons. In the case of the $\tau\mu$ final state the two edges could be guessed, but it will require high luminosity and a finer binning to disentangle the resulting double edge structure due to the contributions of the different sleptons [79].

TABLE I. Edges, as given in Eq. (24), of the invariant lepton masses due to the individual sleptons. The two neutralino masses are 344.6 GeV and 647.0 GeV.

Slepton	Mass (GeV)	$m_{ll'}$ (GeV)
$\tilde{l}_1$	377.9	213.0
$\tilde{l}_{2,3}$	386.0	233.9
$\tilde{l}_4$	621.9	148.3
$\tilde{l}_5$	625.1	139.3
$\tilde{l}_6$	625.9	136.7

IV. CONCLUSIONS

We have studied supersymmetric variants of the seesaw type-III model. At the electroweak scale the particle content is the same as in the MSSM. At the seesaw scale(s) the particles have been included in a **24**-plet to ensure unification of the gauge couplings. In this way one ends up with a combination of the seesaw type-III model and the seesaw type-I model, where the latter gives a subdominant contribution if $SU(5)$-GUT conditions for the corresponding Yukawa couplings are assumed. We have considered two variants of this model using either two or three generations of **24**-plets. The latter case is heavily constrained by the experimental bound on $\mu \to e\gamma$. However, as we have shown there are various ways to obtain cancellations between different contributions, so the bound can be respected: Here the Dirac phase of the neutrino sector enters as does the mass hierarchy of the seesaw particles and their mixing properties. Even though the measurement of the reactor angle θ_{13} gives an additional constraint, the model still has sufficiently many parameters to be consistent with all experimental data. In the two-generation model the constraints due to the rare lepton decays are less severe and can be more easily accommodated.

We have also investigated the question of to which extent lepton flavor violating signals can be seen at the LHC. The current experimental bounds on SUSY particles imply that within a unified model, such as the mSUGRA, squarks and gluinos must be in the TeV range. As the main signal is in the cascade decays of these particles one gets at most a few fb for the signal. This happens for small m_0 and large $m_{1/2}$ if the seesaw parameters are chosen such that BR($\mu \to e\gamma$) is close to its experimental bound. One can turn this around: If the bound BR($\mu \to e\gamma$) is increased by an order of magnitude, then it is rather unlikely that the LHC will find LFV in SUSY decays in this class of models.

ACKNOWLEDGMENTS

We thank J. C. Romão for providing us with his SPHENO FRONTEND which facilitated the scans over the parameter space, and B. O'Leary for providing an updated version of the LHC-FASER package for the cross section calculations. W. P. and Ch. W. thank the IFIC for hospitality during extended stays. Their work has been supported in part by

the DFG Project No. PO-1337/2-1 and the Helmholtz Alliance "Physics at the Terascale." W. P. has been supported by the Alexander von Humboldt Foundation. M. H. acknowledges support from the Spanish MICINN Grants No. FPA2011-22975 and No. MULTIDARK CSD2009-00064, the Generalitat Valenciana Grant No. Prometeo/2009/091, and the EU Network Grant No. UNILHC PITN-GA-2009-237920.

[1] E. Ma, Phys. Rev. Lett. **81**, 1171 (1998).
[2] P. Minkowski, Phys. Lett. **67B**, 421 (1977).
[3] T. Yanagida, *Proceedings of the Workshop on Unified Theory and Baryon Number in the Universe, Tsukuba, Japan, 1979*, edited by O. Sawada and A. Sugamoto (KEK Report no. 79-18, 1979).
[4] M. Gell-Mann, P. Ramond, and R. Slansky, in *Supergravity*, edited by P. van Niewenhuizen and D. Freedman (North Holland, Amsterdam, 1979).
[5] R. N. Mohapatra and G. Senjanovic, Phys. Rev. Lett. **44**, 912 (1980).
[6] J. Schechter and J. Valle, Phys. Rev. D **22**, 2227 (1980).
[7] T. Cheng and L.-F. Li, Phys. Rev. D **22**, 2860 (1980).
[8] R. Foot, H. Lew, X. He, and G. C. Joshi, Z. Phys. C **44**, 441 (1989).
[9] S. Weinberg, Phys. Rev. Lett. **43**, 1566 (1979).
[10] S. Weinberg, Phys. Rev. D **22**, 1694 (1980).
[11] E. Witten, Nucl. Phys. **B188**, 513 (1981).
[12] S. Dimopoulos, S. Raby, and F. Wilczek, Phys. Rev. D **24**, 1681 (1981).
[13] L. E. Ibanez and G. G. Ross, Phys. Lett. **105B**, 439 (1981).
[14] W. J. Marciano and G. Senjanovic, Phys. Rev. D **25**, 3092 (1982).
[15] M. Einhorn and D. Jones, Nucl. Phys. **B196**, 475 (1982).
[16] U. Amaldi, W. de Boer, and H. Furstenau, Phys. Lett. B **260**, 447 (1991).
[17] P. Langacker and M.-x. Luo, Phys. Rev. D **44**, 817 (1991).
[18] J. R. Ellis, S. Kelley, and D. V. Nanopoulos, Phys. Lett. B **260**, 131 (1991).
[19] L. E. Ibanez and G. G. Ross, Phys. Lett. **110B**, 215 (1982).
[20] J. Hisano, M. M. Nojiri, Y. Shimizu, and M. Tanaka, Phys. Rev. D **60**, 055008 (1999).
[21] A. Rossi, Phys. Rev. D **66**, 075003 (2002).
[22] M. R. Buckley and H. Murayama, Phys. Rev. Lett. **97**, 231801 (2006).
[23] M. Hirsch, S. Kaneko, and W. Porod, Phys. Rev. D **78**, 093004 (2008).
[24] F. Borzumati and T. Yamashita, Prog. Theor. Phys. **124**, 761 (2010).
[25] J. Esteves, J. Romão, M. Hirsch, F. Staub, and W. Porod, Phys. Rev. D **83**, 013003 (2011).
[26] F. Borzumati and A. Masiero, Phys. Rev. Lett. **57**, 961 (1986).
[27] J. Hisano, T. Moroi, K. Tobe, M. Yamaguchi, and T. Yanagida, Phys. Lett. B **357**, 579 (1995).
[28] J. Hisano, T. Moroi, K. Tobe, and M. Yamaguchi, Phys. Rev. D **53**, 2442 (1996).
[29] J. R. Ellis, J. Hisano, M. Raidal, and Y. Shimizu, Phys. Rev. D **66**, 115013 (2002).
[30] F. Deppisch, H. Pas, A. Redelbach, R. Rückl, and Y. Shimizu, Eur. Phys. J. C **28**, 365 (2003).
[31] S. Petcov, S. Profumo, Y. Takanishi, and C. Yaguna, Nucl. Phys. **B676**, 453 (2004).
[32] E. Arganda and M. J. Herrero, Phys. Rev. D **73**, 055003 (2006).
[33] S. Petcov, T. Shindou, and Y. Takanishi, Nucl. Phys. **B738**, 219 (2006).
[34] S. Antusch, E. Arganda, M. Herrero, and A. Teixeira, J. High Energy Phys. 11 (2006) 090.
[35] F. Deppisch and J. Valle, Phys. Rev. D **72**, 036001 (2005).
[36] M. Hirsch, J. Valle, W. Porod, J. Romão, and A. V. del Moral, Phys. Rev. D **78**, 013006 (2008).
[37] E. Arganda, M. Herrero, and A. Teixeira, J. High Energy Phys. 10 (2007) 104.
[38] F. Deppisch, T. Kosmas, and J. Valle, Nucl. Phys. **B752**, 80 (2006).
[39] C. Biggio and L. Calibbi, J. High Energy Phys. 10 (2010) 037.
[40] P. F. Perez, Phys. Rev. D **76**, 071701 (2007).
[41] R. Mohapatra, N. Okada, and H.-B. Yu, Phys. Rev. D **78**, 075011 (2008).
[42] A. Abada, A. Figueiredo, J. Romao, and A. Teixeira, J. High Energy Phys. 08 (2011) 099.
[43] G. Aad *et al.* (ATLAS Collaboration), Phys. Lett. B **710**, 49 (2012).
[44] S. Chatrchyan *et al.* (CMS Collaboration), Phys. Lett. B **710**, 26 (2012).
[45] P. Bechtle *et al.*, J. High Energy Phys. 06 (2012) 098.
[46] O. Buchmueller *et al.*, Eur. Phys. J. C **72**, 2243 (2012).
[47] M. Hirsch, F. Joaquim, and A. Vicente, J. High Energy Phys. 11 (2012) 105.
[48] U. Ellwanger and C. Hugonie, Adv. High Energy Phys. **2012**, 625389 (2012).
[49] J. F. Gunion, Y. Jiang, and S. Kraml, Phys. Lett. B **710**, 454 (2012).
[50] G. G. Ross and K. Schmidt-Hoberg, Nucl. Phys. **B862**, 710 (2012).
[51] U. Ellwanger, C. Hugonie, and A. M. Teixeira, Phys. Rep. **496**, 1 (2010).
[52] S. Choi, D. J. Miller, and P. Zerwas, Nucl. Phys. **B711**, 83 (2005).
[53] C. Cheung, L. J. Hall, D. Pinner, and J. T. Ruderman, arXiv:1211.4873.
[54] A. Delgado, C. Kolda, and A. de la Puente, Phys. Lett. B **710**, 460 (2012).
[55] G. G. Ross, K. Schmidt-Hoberg, and F. Staub, J. High Energy Phys. 08 (2012) 074.

[56] S. K. Kang, T. Morozumi, and N. Yokozaki, J. High Energy Phys. 11 (2010) 061.
[57] J. Casas and A. Ibarra, Nucl. Phys. **B618**, 171 (2001).
[58] A. Ibarra and G. G. Ross, Phys. Lett. B **591**, 285 (2004).
[59] P. H. Chankowski, J. R. Ellis, S. Pokorski, M. Raidal, and K. Turzynski, Nucl. Phys. **B690**, 279 (2004).
[60] B. Dutta and R. N. Mohapatra, Phys. Rev. D **68**, 056006 (2003).
[61] Special issue on Neutrino Physics, edited by F. Halzen, M. Lindner, and A. Suzuki, [New J. Phys. **6**, 202 (2004)].
[62] A. Ibarra, J. High Energy Phys. 01 (2006) 064.
[63] A. Bartl, W. Majerotto, W. Porod, and D. Wyler, Phys. Rev. D **68**, 053005 (2003).
[64] W. Porod, Comput. Phys. Commun. **153**, 275 (2003).
[65] W. Porod and F. Staub, Comput. Phys. Commun. **183**, 2458 (2012).
[66] F. Staub, arXiv:0806.0538.
[67] F. Staub, Comput. Phys. Commun. **181**, 1077 (2010).
[68] F. Staub, Comput. Phys. Commun. **182**, 808 (2011).
[69] F. Staub, arXiv:1207.0906.
[70] F. Staub, T. Ohl, W. Porod, and C. Speckner, Comput. Phys. Commun. **183**, 2165 (2012).
[71] W. Kilian, T. Ohl, and J. Reuter, Eur. Phys. J. C **71**, 1742 (2011).
[72] D. Forero, M. Tortola, and J. Valle, Phys. Rev. D **86**, 073012 (2012).
[73] J. Adam *et al.* (MEG Collaboration), Phys. Rev. Lett. **107**, 171801 (2011).
[74] F. An *et al.* (Daya Bay Collaboration), Phys. Rev. Lett. **108**, 171803 (2012).
[75] J. Ahn *et al.* (RENO Collaboration), Phys. Rev. Lett. **108**, 191802 (2012).
[76] L. Calibbi, D. Chowdhury, A. Masiero, K. Patel, and S. Vempati, J. High Energy Phys. 11 (2012) 040.
[77] I. Hinchliffe and F. Paige, Phys. Rev. D **63**, 115006 (2001).
[78] F. Deppisch, J. Kalinowski, H. Pas, A. Redelbach, and R. Rückl, arXiv:hep-ph/0401243.
[79] A. Bartl, K. Hidaka, K. Hohenwarter-Sodek, T. Kernreiter, W. Majerotto, and W. Porod, Eur. Phys. J. C **46**, 783 (2006).
[80] Y. Andreev, S. Bityukov, N. Krasnikov, and A. Toropin, Phys. At. Nucl. **70**, 1717 (2007).
[81] F. del Aguila *et al.*, Eur. Phys. J. C **57**, 183 (2008).
[82] E. Carquin, J. Ellis, M. Gomez, S. Lola, and J. Rodriguez-Quintero, J. High Energy Phys. 05 (2009) 026.
[83] J. Esteves, M. Hirsch, W. Porod, J. C. Romao, J. W. F. Valle, and A. V. del Moral, J. High Energy Phys. 05 (2009) 003.
[84] W. Beenakker, S. Brensing, M. Krämer, A. Kulesza, E. Laenen, and I. Niessen, J. High Energy Phys. 01 (2012) 076.
[85] M. Kramer *et al.*, arXiv:1206.2892.
[86] W. Hollik, J. M. Lindert, and D. Pagani, arXiv:1207.1071.
[87] U. Langenfeld, S.-O. Moch, and T. Pfoh, J. High Energy Phys. 11 (2012) 070.
[88] S. Chatrchyan *et al.* (CMS Collaboration), J. High Energy Phys. 10 (2012) 018.
[89] S. Chatrchyan *et al.* (CMS Collaboration), Phys. Rev. Lett. **109**, 171803 (2012).
[90] G. Aad *et al.* (ATLAS Collaboration), arXiv:1208.0949.
[91] G. Aad *et al.* (ATLAS Collaboration), Phys. Rev. D **86**, 092002 (2012).
[92] H. K. Dreiner, M. Kramer, J. M. Lindert, and B. O'Leary, J. High Energy Phys. 04 (2010) 109.
[93] B. O'Leary, LHC-FASER, https://github.com/benoleary/LHC-FASER, 2012.
[94] J. Hisano, R. Kitano, and M. M. Nojiri, Phys. Rev. D **65**, 116002 (2002).
[95] J. Harz, Diploma thesis, University of Würzburg, 2010.